Microenvironmental Modification by Small Water Droplet Evaporation

FRED V. NURNBERGER[1] AND GEORGE E. MERVA

Agricultural Engineering Department, Michigan State University, East Lansing 48823

JAMES B. HARRINGTON, JR.

Forest Fire Research Institute, Canadian Forestry Service, Ottawa, Ontario, Canada

(Manuscript received 18 November 1974 and 20 February 1976 as Parts I and II, in revised consolidated form 1 June 1976)

ABSTRACT

A mathematical model is developed to predict the microclimatic modification of air near the ground by the evaporation of an ultrafine water mist. The model equations with realistic parameters and boundary values are solved using the Patankar and Spalding control volume integral technique. The reported field experiment provides reasonable preliminary confirmation of the model. The maximum predicted cooling under the conditions tested is −14.6°C.

1. Introduction

Evaporative cooling techniques are commonly used to air condition enclosed spaces (Esmay, 1969; Shaw, 1967), and in some parts of the southwestern United States the techniques are used to air condition domestic animal feedlots (Shaw, 1967).

There have been, however, few theoretical studies designed to determine the feasibility and limits of outdoor air conditioning generally and no adequately controlled experiments to test the theoretical models.

Extensive potential applications in agriculture include the possibility of reducing the use of irrigation water and increasing plant yield by reducing temperature damage during the hot hours of the day (Carolus, *et al.*, 1965; Van Den Brink and Carolus, 1965; Bible, *et al.*, 1968; Carolus, 1967, 1969), increasing the productivity of domesticated animals by reducing heat stress (Shaw, 1967), and perhaps even reducing soil drifting on muck and other light soils by stabilizing the lowest few meters of the atmosphere. Outdoor air conditioning also has great potential value in increasing human comfort in hot urban centers, particularly in malls and shopping centers. The advantage of using ultrafine water mist is that its rapid evaporation prevents the deposition of liquid water, thereby reducing the possibility of disease in plants and discomfort of animals and man.

2. Model development

Consider an infinite horizontal homogeneous plain whose surface is impervious to the passage of water vapor and positioned above it an infinite line source of water mist located at height z_{ms}. If steady state is assumed and the downwind diffusion neglected in comparison with downwind transport, the diffusion equations for liquid water, water vapor and heat can be written, respectively, as

$$u(z)\frac{\partial c}{\partial x}=\frac{\partial}{\partial z}\left[K_c(z)\frac{\partial c}{\partial z}+\bar{q}c\right]+\Phi_c(z,x), \tag{1}$$

$$u(z)\frac{\partial \chi}{\partial x}=\frac{\partial}{\partial z}\left[K_\chi(z)\frac{\partial \chi}{\partial z}\right]+\Phi_\chi(z,x), \tag{2}$$

$$u(z)\frac{\partial T}{\partial x}=\frac{\partial}{\partial z}\left[K_H(z)\frac{\partial T}{\partial z}\right]+\frac{1}{\rho c_p}\Phi_H(z,x), \tag{3}$$

where $\bar{q}$ is the mean settling speed of the water drops, $\Phi(z,x)$ a source term for the diffusing quantities, and the other symbols have their usual meaning.[2] These equations are linked by the source term $\Phi(z,x)$ and by the possible influence of the temperature profile on wind speed and diffusivity profiles. Their simultaneous solution can be determined numerically if the parametric values can be estimated or computed and if the initial and boundary values are known. To simplify the model in these initial solutions, the wind speed and diffusivity profiles are assumed to be unchanged by the evaporation of the liquid water and the mean settling speed of the liquid drops is assumed to be zero. Thus Eqs. (1)–(3) reduce to the same form

$$u(z)\frac{\partial \phi}{\partial x}=\frac{\partial}{\partial z}\left[K(z)\frac{\partial \phi}{\partial z}\right]+\Phi(z,x), \tag{4}$$

where ϕ is the arbitrary dependent variable.

[1] Also Michigan Department of Agriculture/Weather Service.

[2] A list of symbols is given in an appendix.

The solution space is limited to the lower 10 m of the atmosphere where the shear stress is nearly constant with height and where profile-gradient techniques can be used to determine fluxes with considerable accuracy (Monin and Yaglom, 1971, pp. 423 and 509). This region lies almost completely within the thermal sublayer (Priestley, 1955; Yordanov, 1966) and therefore a single layer model is appropriate. Following the extensive examination by Harrington (1965) of various profile formulations, the wind speed and momentum diffusivity profiles are expressed using the exponential laws proposed by Swinbank (1964). These equations are a convenient approximation to the Monin-Obukhov log-plus-linear law for values of Ri near zero and are more suitable during conditions of large negative Ri experienced during clear days. The Swinbank profiles of wind speed and momentum diffusivity are

$$u(z)=\frac{u_*}{k}\ln\left[\frac{\exp(\zeta)-1}{\exp(\zeta_0)-1}\right], \tag{5}$$

$$K_M(z)=ku_*L[1-\exp(-\zeta)], \tag{6}$$

where

$$L\equiv\frac{-u_*^3}{\frac{kg}{T_A}\frac{H}{\rho c_p}},$$

T_A is the absolute temperature, $\zeta=z/L$, $\zeta_0=z_0/L$, and the other symbols have their usual meanings.

Under the similarity theory developed by Monin and Obukhov (1954) and expressed in Lumley and Panofsky (1964, pp. 99–116), Monin and Yaglom (1971, p. 487), and others, the unmodified temperature and moisture profiles should have a form mathematically similar to that of the wind velocity profile. These can then be expressed as

$$T=T_0-T_*\ln\left[\frac{\exp(\zeta)-1}{\exp(\zeta_0)-1}\right], \tag{7}$$

$$\chi=\chi_0-\chi_*\ln\left[\frac{\exp(\zeta)-1}{\exp(\zeta_0)-1}\right], \tag{8}$$

where

$$T_*=\frac{-H_0}{\alpha_0 ku_*\rho c_p},$$

$$\chi_*=\frac{-E_0}{\alpha_0 ku_*}.$$

Monin and Yaglom (1971, p. 442) concluded that the diffusivities for heat and water vapor under unstable conditions are approximately equal. The ratios of thermal and water vapor diffusivities to that for momentum are assumed to be approximated by the Leichtmann and Ponomareva (1969) form

$$\alpha_H=\frac{K_H}{K_M}=\begin{cases}0.8, & \text{for } -0.03<\zeta\leqslant+0.10\\ 3.2|\zeta|^{0.35}, & \text{for } -0.8<\zeta\leqslant-0.03\\ 3.0, & \text{for } \zeta\leqslant-0.8\end{cases} \tag{9}$$

The liquid water source term Φ_c and the related terms for water vapor and heat, Φ_χ and Φ_H, require a knowledge of the evaporation rate of fine water droplets under varying atmospheric conditions. From a review of the complex and sometimes unverified droplet evaporation models proposed by Milburn (1957, 1958), Okuyama and Zung (1967), Zung (1967a, b; 1968) and others, the modified Fuchs-Okuyama-Zung (FOZ) model (Zung, 1967a, p. 2066) was selected. For a monodispersed system of uniform drop size the source term using the FOZ model can be approximated as

$$\Phi_c=c_1(\chi_s-\chi), \tag{10}$$

where c_1 is the coefficient of evaporation, χ_s the saturated water vapor concentration, and χ the ambient water vapor concentration.

A simple initial liquid water concentration pattern was selected to approximate the discharge from elevated mist nozzles. The assumed initial distribution of liquid water mist was a sawtooth pattern written in the form

$$c_i(z)=\frac{W(z)S}{u(z)\Delta z}, \tag{11}$$

where S is the spray rate per meter of line, $W(z)$ the weighting distribution function chosen such that the integral of the density function over the droplet distribution is properly unity, and the others as previously defined.

The lower boundary condition has been greatly simplified by assuming a zero flux of liquid water and water vapor, maintained mathematically by the method of images. The sensible heat flux H_0 is determined by the energy balance method. With no evaporation or transpiration at the surface, the energy balance is simply

$$H_0=R_N-G, \tag{12}$$

where the usual sign conventions have been used.

The upper boundary is taken at a sufficient elevation to afford no change in the initial conditions.

3. Method of solution

The simultaneous solution of (1), (2) and (3) is carried out by a numerical method proposed by Patankar and Spalding (1968) and discussed further in Patankar and Spalding (1970). For problems with variable coefficients, this method is both faster and simpler than the usual finite-difference approach such as the methods discussed by Smith (1965), Richtmyer

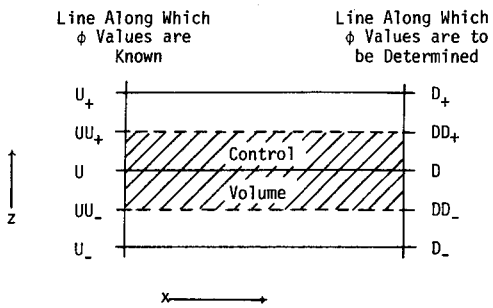

FIG. 1. Patankar-Spalding grid and control volume. U and D represent upwind and downwind grid points. Double letters represent internode midpoints. Subscripts represent grid points above (+) and below (−) the solution points.

and Morton (1967), and by many others. The Patankar-Spalding technique uses an integral equation over a control volume coupled with the assumption that the dependent variable changes linearly between solution nodes in the vertical direction and stepwise in the downstream direction. One additional principal advantage of this integral-control volume technique is its ability to ensure that the conservation equation remains satisfied over any part of the boundary layer (Patankar and Spalding, 1968, p. 35). The solution grid and control volume are shown in Fig. 1.

The general Patankar-Spalding technique permits the use of variable node spacing in all directions. In the work presented here, however, the use of Simpson's rule for integration during the development of the equations restricts the nodal points to a uniform grid. The choice of Simpson's rule is based upon the reduced truncation error compared to that of the trapezoidal rule (Hamming, 1962; Korn and Korn, 1968). The increased complexity caused by using more sophisticated integration techniques (Abramowitz and Stegun, 1965) is not deemed justified. The loss of the more general formulation allowing variable node spacing with the original trapezoidal rule used in the Patankar-Spalding development is not considered significant for this investigation.

Following Patankar and Spalding's procedures, the following steps and assumptions are made in this mathematical development. A more detailed development is given by Nurnberger (1972).

1) Eq. (4) is rearranged to isolate $\partial\phi/\partial x$ on the left-hand side.

2) Each term of the resulting partial differential equation is expressed as an integrated average over the control volume given in Fig. 1.

3) Evaluation of the $\partial/\partial z$ terms is accomplished by using the ϕ values at x_D.

4) The coefficients are evaluated from the known upstream values of ϕ at x_U.

5) The dependent variable ϕ is assumed linear with respect to z between grid points and as a step function with respect to x.

6) The wind profile and diffusivities are assumed to remain unchanged from the initial conditions.

7) Development of the flux term requires an intermediate step of integration by parts and then the resulting expression is evaluated numerically by Simpson's rule as previously mentioned.

8) For N grid points, the resulting set of equations consists of N independent equations in $N+2$ unknowns, but with two additional independent equations obtained from the boundary conditions a unique solution is assured.

9) The Gaussian elimination method is applied to the resulting set of equations to obtain the final form of the solution, $\phi_i = A_i\phi_{i+1} + B_i$.

The final solution form is identical to that presented by Patankar and Spalding (1968, p. 45) and as noted by them "The computing time needed for these calculations is directly proportional to the number of ϕ's which are to be determined; standard matrix-inversion techniques, by contrast, require a computation time proportional to N^2 or N^3."

Similar equations are developed for each of the three variables liquid water, water vapor and temperature. The liquid water concentration equation is solved first, the temperature (energy) equation second, and the absolute humidity equation third with coupling occurring through the source terms. The process is repeated at each downwind step. Checks are made to ensure that local saturation conditions are not exceeded.

4. Parameter evaluation

The temperature range of applicability of the model is from 20 to 50°C, since this range extends beyond the active plant growing temperature extremes for which cooling would be desirable (Wang, 1972, p. 108). The ambient relative humidity conditions will range from low values at the high temperatures to near-saturation values at the low temperatures. An examination of the relevant parameters over the temperature and humidity ranges given above lead to the following conclusions:

1) The deviation of moist air from an ideal gas is negligible (a common assumption).

2) The evaporative cooling rate will be on the order of 2°C per gram of water evaporated per cubic meter of air.

3) The maximum cooling under normal conditions will be less than 20°C.

4) The moist air density, isobaric specific heat, latent heat of vaporization, heat capacity, and evaporative cooling rate can all be assumed constant and evaluated at an intermediate value within the range of conditions applicable to a specific problem.

The errors incurred will be less than the maximum of ~3% for the extreme conditions of initially 50°C air cooled to 30°C. Thus the implied assumption in the

development of Eq. (3), that ρc_p = constant, is justified. A check of continuity of all three variable profiles at each solution step revealed an error of less than 0.5% of the total integrated value for each profile. Computational errors for the model were estimated to be less than 1%.

5. Field experiment

The following field experiment was designed to test the theoretical model and to determine the practicality of its potential use in predicting the heat stress relief for plants, animals and humans.

The experimental site was located on a level muck area at the Michigan State University Experimental Muck Farm (84°23′W, 42°50′N), approximately 15 km northeast of the city of East Lansing. The site itself was a square grass covered field 16.2 hectares (40 acres) in area with other experimental fields upwind of the site as shown in Fig. 2a. Low pine windbreaks located 0.8 km or more from the experimental site traversed some of the fields. The entire farm is fringed by trees which were estimated to have an average height of about 20 m giving a minimum fetch to tree height ratio of approximately 20:1, adequate to establish profile similarity (Brooks, 1961).

A 300 m by 120 m strip was plowed diagonally across the site, tilled, smoothed, and chemically treated to kill

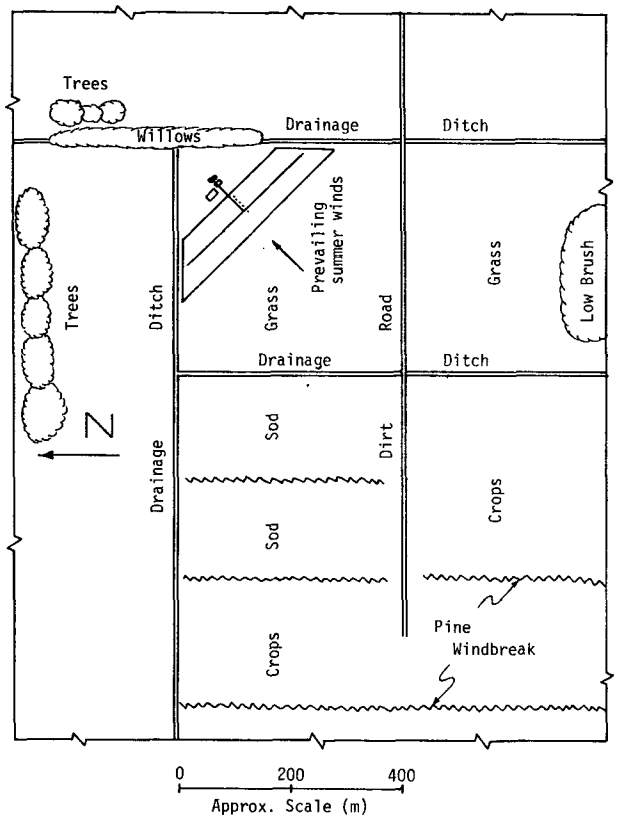

FIG. 2a. Schematic diagram of the experimental site.

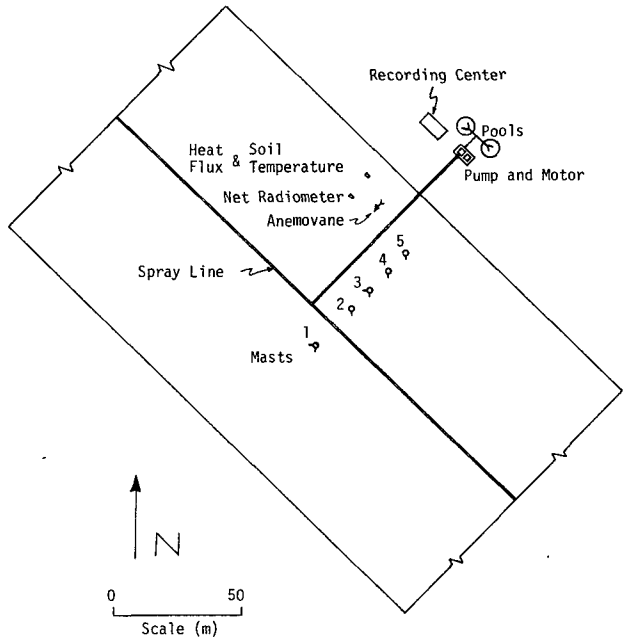

FIG. 2b. Schematic diagram of the instrumentation and spray line.

all vegetation. A spray line positioned along the centerline of the strip approximated an infinite line source so that observations of micrometeorological modification were measurable along a single line normal to the source, thus satisfying the two-dimensional mathematical model. When dry, the surface of the treated area became a light-weight, powdery, almost impermeable barrier to heat and water vapor. The ratio of the fetch over the bare strip to the upwind grass height was better than 200:1, in agreement with the suggestions of Inoue *et al.* (1958).

The spray line consisted of a base feeder of standard 3-inch aluminum irrigation pipe with welded couplings and standard $\frac{3}{4}$-inch galvanized steel pipe risers supplying an elevated $\frac{3}{4}$-inch line at a height of one meter. The elevated line was equipped with Bette fog nozzles which were selected to supply drops in the 20–50 μm range under the obtainable line pressures and spaced at intervals of 0.67 m. The spray rate of the completed assembly was measured by collecting each nozzle's discharge into a graduated cylinder for three 1 min time periods and averaging the results.

Water was supplied to the center of the spray line by the irrigation pipe mentioned above at a gage pressure of 8.8 kgwt cm^{-2} (125 psi) from a pump located downwind of the treated area, as shown in Fig. 2b. Two above-ground reservoirs, approximately 30 m^3 each, were used to provide water of a constant temperature.

The instruments for measuring the vertical profiles of temperature, moisture and wind speed were mounted on 9.1 m masts. Five masts were erected perpendicular to the center of the spray line, the first located 10 m upwind from the spray line and masts two through five positioned at 10 m intervals downwind (Fig. 2b). Wind

speed was measured at the 1, 2, 4 and 8 m levels on masts one and three using Climet 3-cup anemometers, model 011-1. Temperature and moisture profiles were measured at the 1, 2, 4, 6 and 8 m levels on all masts by means of aspirated thermistor psychrometers. The thermistors had an accuracy of ± 0.15°C with a still air time constant of 10 s. All thermistors were shielded from solar radiation and water for the wet thermistor was supplied by a wick leading to a constant water level chamber. Data were processed and punched on paper tape twice per minute for each of the 68 input signals.

Wind direction was measured with a Climet anemovane, net radiation by a Beckman-Whitley net radiometer, and soil heat flux by a Thornthwaite heat-flux plate placed at the ground surface beneath a thin ($\sim$1–2 mm) layer of soil. The signals were recorded by strip chart recorders.

The ground temperature profile was measured at equal intervals of 2.5 cm at a depth of 60 cm by copper-constantan thermocouples and a 24-point recorder. The uppermost thermocouple was located at the ground surface and covered by a thin ($\sim$1–2 mm) layer of soil.

6. Results

a. Field test

The following experimental test was run under a cloudless sky for $1\frac{1}{2}$ h from 1230–1400 EST 12 September 1970. All observed initial profile data were compared to the Swinbank (1964) profiles given by Eqs. (5), (7) and (8). Values of the various measured and computed parameters are given in Table 1. Unless otherwise noted, all quantities are 30 min averages.

Photographs looking along the spray line are shown in Fig. 3. Despite the initial downward orientation of the spray, the lack of significant inertia in the drops allowed them to rapidly attain equilibrium with the momentum of the air. The point at which liquid water droplets visually disappeared was between masts two and three downwind from the spray line. This location agreed with the model predicted distance for persistence of liquid water, namely 23 m.

TABLE 1. Parametric values for the micrometeorological modification test site near East Lansing, Mich., 12 September 1970.

Time	1230–1400 EST
Solar noon	1234 EST
Ambient pressure P	984.8 mb
Ambient density ρ	1.15 kg m^{-3}
Elevation above MSL	250 m
Wind direction (25° from normal to sprayline)	200° from N
Roughness length z_0	1.6 mm
Friction velocity u_*	0.28 m s^{-1}
Scale length L	−1.66 m
Net radiation R_N	0.27 ly min^{-1}
Soil heat flux G	0.14 ly min^{-1}
Sensible heat flux H_0	0.13 ly min^{-1}
Soil surface temperature	24.5°C
Scale temperature T_*	−0.869°C
Scale humidity χ_*	−1.66 g m^{-3}
Spray rate S	8.0 g m^{-1} s^{-1}

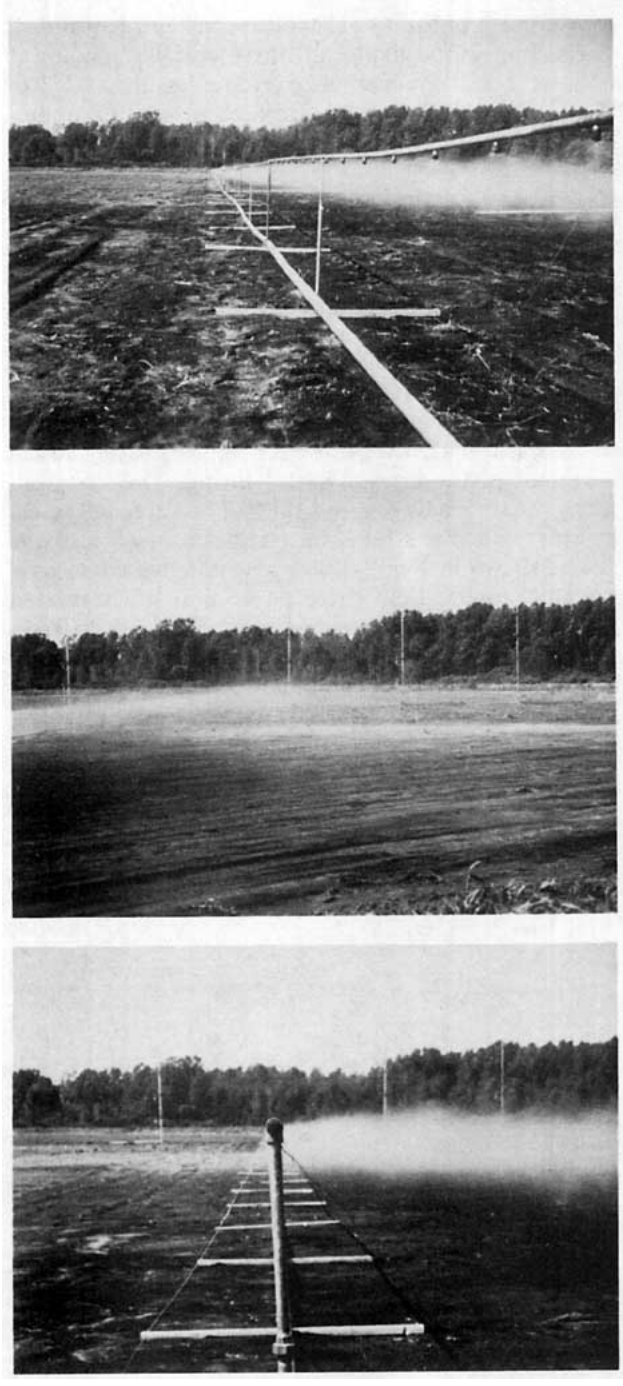

FIG. 3. Field operations from views oblique to the spray line (top), normal to the line (middle) and along the spray line (bottom).

Fig. 4 shows that the wind speed profiles on masts one and three show reasonable agreement with the Swinbank (1964) model. No significant difference exists between the upwind profile at mast one and the downwind profile at mast three, suggesting that any modifica-

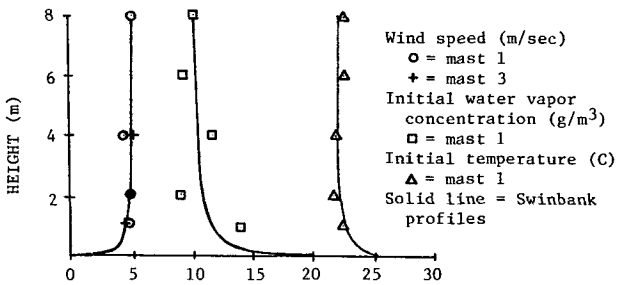

FIG. 4. Average wind speed, initial water vapor concentration and initial temperature profiles.

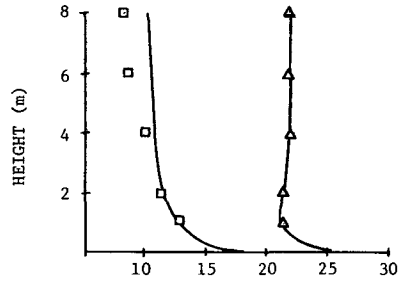

FIG. 6. Water vapor concentration and temperature profiles at mast 3.

tion in atmospheric stability had not yet had time to affect the wind. This was not surprising because the time scale of the turbulence, L/u_*, was approximately 6 s and the wind at approximately 5 m s^{-1} would have already reached the fourth mast.

The Swinbank initial temperature and water vapor concentration (absolute humidity) profiles, computed using the minimum sum of squared errors technique (Himmelblau, 1970), are also compared to the measured values in Fig. 4. The computed temperatures below 4 m are overestimated while those above 4 m are underestimated. The absolute humidity data failed to define a clear profile. The minimum sum of squared errors for the temperature and absolute humidity were 0.871 and 13.1, respectively.

Although the absolute humidity data were inferior to the temperature profile data, as evidenced by the lack of agreement between the observed and the computed values, a strong consistency exists between the humidity profiles. The marked bulge in these profiles at 4 m is undoubtedly a transition from the boundary layer associated with the relatively dry bare soil into the boundary layer associated with the transpiring grass. Instead of a single profile through the data, a much better fit could be obtained by drawing a separate curve for each regime with a fairly sharp transition zone between them (Tennekes and Lumley, 1972, p. 192). This concept was approximated in the model tests by "linearizing" the initial conditions as connected straight line segments between observed data points (Fig. 5).

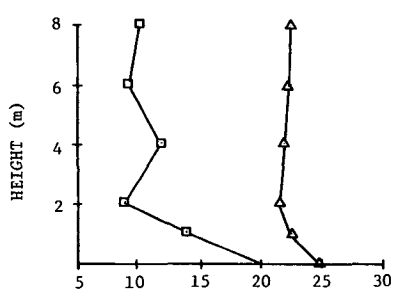

FIG. 5. "Linearized" initial water vapor concentration and temperature profiles.

Comparisons between the computed and observed temperature and water vapor concentration profiles at two downwind masts, using the "linearized" initial conditions, are shown in Figs. 6 and 7. The sums of the squared errors between the computed and observed profiles are given for all masts in Table 2. The maximum cooling predicted by the model was −1.02°C at 19.0 m downwind and at a height of 0.67 m. This is in good agreement with the observed temperature at mast three, 22.1 m downwind from the spray line (Fig. 6).

b. Model predictions

The model was used to obtain predicted cooling levels for a reasonable range of each of the parametric values. Figs. 8 and 9 are the temperature and moisture concentration profiles, respectively, for the parametric values given in Table 3. Curve A is the initial condition and curve B the downstream location of maximum cooling. The maximum predicted cooling for these conditions is −9.5°C at 19.0 m downstream at a height of 0.15 m.

Table 4 gives the values of the Monin-Obukhov stability factor L, the initial temperature at 1 m, $T_i(1)$, the initial wind speed at 1 m, $u_i(1)$, and the spray rate, which are used in the model for computation of various cooling levels. All other parameters given in Table 1 remain constant. Not all combinations of the four adjustable parameters are utilized, however, since the combinations for $u_i \geqslant 2.0$ m s^{-1} and $L = -0.1$ produce impossible requirements for the sensible heat flux to be consistent with L, u_* and T_*. For example, in the 30–40°C temperature range, H would be required to have

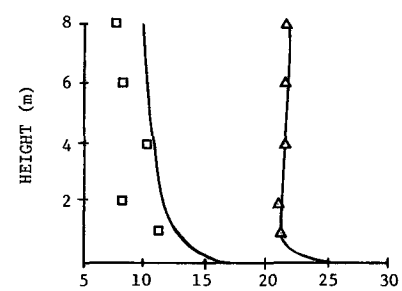

FIG. 7. As in Fig. 6 except at mast 4.

TABLE 2. Sum of the squared errors between computed and observed profiles using linear interpolation between observed values as initial conditions.

Profile	Mast number 1	2	3	4	5
Temperature (°C)²	0	0.33	0.03	0.16	0.57
Moisture (g m⁻³)²	0	5.68	6.27	20.00	5.86

a value nearly three times the solar constant. These combinations were therefore omitted.

Figs. 10–13 give the results of the model predictions for each selected initial wind speed in the form of maximum cooling vs initial temperature at the 1 m height for the three selected spray rates. The actual values of the parameters producing the maximum cooling and the locations of the maximum cooling are given in Table 5. The maximum cooling for all the conditions tested is −14.6°C at 41.0 m downstream, at a height of 1.25 m, for T_i=40.0°C, u_i=0.5 m s^{-1}, L=−10.0 m, and a spray rate per meter of line of 20.0 g m^{-1} s^{-1}. The maximum cooling value is well within the expected range stated above.

7. Conclusions

From an inspection of Figs. 10–13 and Table 5, one may conclude that:

1) The maximum cooling occurs with the lowest wind speed and highest initial temperature, spray rate and instability.

2) The rate of change in the maximum cooling with respect to the initial temperature is reduced with increasing wind speed.

3) The variation in maximum cooling with spray rates is wind-speed dependent.

4) The height of the point of maximum cooling and its associated distance downwind from the source both generally become smaller as wind speed increases.

5) The distance downstream for maximum cooling increases with both increasing spray rate and decreasing initial temperature.

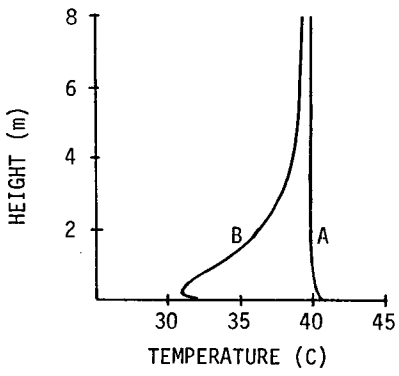

FIG. 8. Predicted temperature profiles.

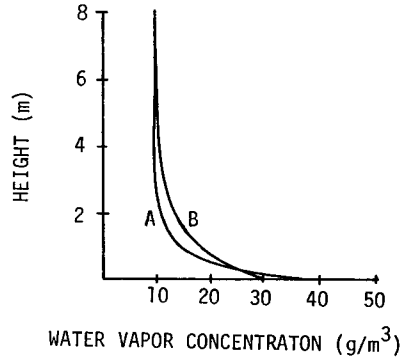

FIG. 9. Predicted water vapor concentration profiles.

All are consistent with the physical processes governing turbulent diffusion and evaporation.

The results indicate that outdoor air conditioning is possible under a broad range of meteorological conditions. The greatest cooling is obtained on days with high temperatures and light winds. Under extreme conditions, cooling in the lowest 1–2 m resulting from the evaporation of mist from a single line located 1 m above the ground could exceed 10°C. Such cooling is more than would be required to relieve heat stress under these conditions.

8. Discussion and recommendations

The model was developed under the assumption of zero flux of liquid water and water vapor at the surface with the condition maintained through the method of images. These simplified boundary conditions, however, resulted in a discontinuity of the temperature profile at the surface as computed by the model and compared to that measured by the soil surface thermocouple. Since the surface of the site during the tests was not

TABLE 3. Parametric values used in the model solution results depicted in Figs. 8 and 9.

L=−1.0 m	c_1=0.02 s^{-1}
$u_i(1)$=2.0 m s^{-1}	P=1000 mb
$T_i(1)$=40°C	z_0=0.01 m
Spray=20.0 g m^{-1} s^{-1}	z_2=0.4 m
RH$_i$(1)=0.25	z_{ms}=0.6 m
ρ=1.12 kg m^{-3}	z_3=0.8 m
L_v=580.0 cal g^{-1}	$\Delta\zeta$=0.1
c_p=0.250 cal g^{-1} °C	Δx=1.0 m

TABLE 4. Values of L, $T_i(1)$, $u_i(1)$, and the spray rate used in the prediction model.

Variable	Values			
L, m	−0.1	−1.0	−10.0	
$T_i(1)$, °C	30.0	35.0	40.0	
$u_i(1)$, m s^{-1}	0.5	1.0	2.0	4.0
Spray rate, g m^{-1} s^{-1}	10.0	15.0	20.0	

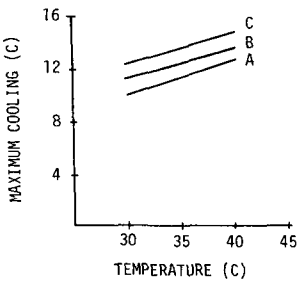

FIG. 10. Predicted maximum cooling vs initial temperature at 1 m for u_i=0.5 m s^{-1} and three spray rates.

dry, evaporation was occurring so that the energy balance used in the model overestimated the sensible heat because the water vapor and latent energy fluxes were ignored. An overestimate of the value of the sensible heat flux would lead to a conservative estimate of the cooling. Since the main objective of this phase of the project was to test the modification concept under simplified conditions, the error was not deemed critical.

The authors could not completely explain the observed unusual temperature profile. Increasing temperatures with height above 10 or 20 m have been noted by various authors but there are no recorded observations of such low-level daytime inversions over homogeneous terrain during strong insolation. Over heterogeneous terrain, a possibility that the profile extended through a developing boundary layer into the boundary layer of a different upwind surface may have occurred. That situation may have applied to these observations because the bare muck soil extended only 60 m normal (66 m in the wind direction) to the spray line.

Some deviations between the computed and measured temperatures occurred at mast two, within the droplet evaporation region. These were attributed to the combined effects of the approximate nature of the

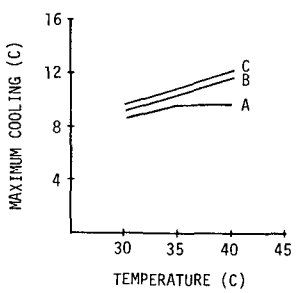

FIG. 11. As in Fig. 10 except for u_i=1.0 m s^{-1}.

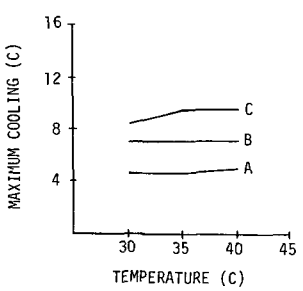

FIG. 12. As in Fig. 10 except for u_i=2.0 m s^{-1}.

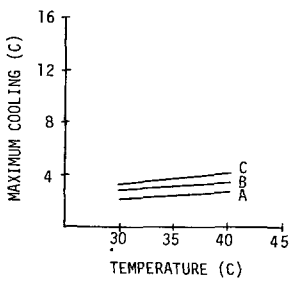

FIG. 13. As in Fig. 10 except for u_i=4.0 m s^{-1}.

TABLE 5. Magnitude and location of the predicted maximum cooling for selected combinations of parametric values.

Spray (g m^{-1} s^{-1})	T_i (°C)	Maximum cooling L (m)	ΔT (°C)	x (m)	z (m)
For u_i=0.5 m s^{-1}					
10	30	−1.0	−10.0	16.0	0.75
	35	−1.0	−11.3	15.0	0.15
	40	−1.0	−12.4	13.0	0.55
15	30	−10.0	−11.3	43.0	1.05
	35	−10.0	−12.3	38.0	0.95
	40	−1.0	−13.4	16.0	0.85
20	30	−10.0	−12.3	53.0	1.55
	35	−10.0	−13.4	46.0	1.35
	40	−10.0	−14.6	41.0	1.25
For u_i=1.0 m s^{-1}					
10	30	−1.0	−8.5	17.0	0.25
	35	−1.0	−9.5	15.0	0.15
	40	−1.0	−9.6	13.0	0.15
15	30	−1.0	−9.0	20.0	0.55
	35	−1.0	−10.3	19.0	0.45
	40	−1.0	−11.4	17.0	0.35
20	30	−10.0	−9.6	42.0	0.35
	35	−1.0	−10.7	21.0	0.65
	40	−1.0	−12.0	19.0	0.55
For u_i=2.0 m s^{-1}					
10	30	−1.0	−4.7	15.0	0.15
	35	−1.0	−4.6	13.0	0.15
	40	−10.0	−5.0	13.0	0.35
15	30	−1.0	−7.1	20.0	0.15
	35	−1.0	−7.1	17.0	0.15
	40	−1.0	−7.1	15.0	0.15
20	30	−1.0	−8.4	21.0	0.15
	35	−1.0	−9.5	23.0	0.15
	40	−1.0	−9.5	19.0	0.15
For u_i=4.0 m s^{-1}					
10	30	−10.0	−2.2	15.0	0.45
	35	−10.0	−2.4	13.0	0.45
	40	−10.0	−2.7	11.0	0.45
15	30	−10.0	−2.8	20.0	0.45
	35	−10.0	−3.1	17.0	0.45
	40	−10.0	−3.4	15.0	0.45
20	30	−10.0	−3.3	25.0	0.35
	35	−10.0	−3.7	21.0	0.35
	40	−10.0	−4.1	18.0	0.35

FOZ droplet evaporation expression [Eq. (10)] and the influence of the evaporating liquid water droplets passing over the temperature sensing elements during aspiration.

The disagreement between computed and observed moisture profiles was believed to be due to the inaccuracy of the observations. The poorest agreement occurred between the model and the observed moisture profiles at mast four. This effect was observed in preliminary tests and persisted despite a change of instrumentation at the mast. The cause of this deviation is unknown. Nothing in the observations, however, confutes the results of the model predictions with respect to temperature, i.e., amount of cooling.

The authors regard the results of the field test as preliminary in nature. However, due to uncontrollable circumstances and the curtailment of research funding, no complete mid-summer operational tests were conducted. Further evaluation of the model is recommended with additional measurements taken below 1 m.

The simplified model must be modified if it is to be used to include other factors such as large water droplet deposition and plant canopies. The inclusion of large water droplets would require the fall rates and different evaporation coefficients of the drops to be taken into account as well as the moisture and latent heat fluxes at the lower boundary. The redevelopment of the model with a plant canopy at the lower boundary, requiring the inclusion of the moisture and latent heat fluxes, is not believed particularly difficult. The complexity of the problem lies in the experimental verification of the flux terms at the "surface" of the plant canopy. These latter conditions are all beyond the scope of the present investigation.

Acknowledgments. The authors wish to acknowledge and thank the following supporters, without whose assistance this project would not have been possible:

Michigan State University Department of Agricultural Engineering
Michigan State University Department of Water Resources
Michigan State University Department of Soil Science/Experimental Muck Farm
Consumers Power Company
Dow Chemical Company
John Bean Division of Food Machinery Corporation.

In addition, appreciation is extended to all the graduate students, undergraduate students, family and friends who "volunteered" their efforts to the entire project.

Our special thanks to Maxine Oshel for typing the manuscript.

APPENDIX

List of Symbols

c	contaminant (liquid water) concentration
$c_i(z)$	initial liquid water concentration profile
c_1	evaporation source term coefficient
c_p	isobaric specific heat
g	acceleration of gravity
k	von Kármán's constant
$\bar{q}$	average gravitational settling speed of the water droplets
$u(z)$	wind speed in the direction of mean flow
$u_i(1)$	initial wind speed at the 1 m level
u_*	friction velocity
x	direction along the mean wind
Δx	solution increment in the x direction
z	height
z_{ms}	location of the maximum initial liquid water concentration
z_0	surface roughness height
z_2	bottom vertex of initial liquid water concentration profile
z_3	top vertex of initial liquid water concentration profile
Δz	vertical node spacing
A	Patankar-Spalding solution coefficient
B	Patankar-Spalding solution coefficient
D	downstream solution node
DD	midpoint between vertically adjacent downstream nodes
E_0	moisture flux at the height z_0
G	soil heat flux
H	sensible heat flux
H_0	sensible heat flux at the height z_0
$K(z)$	turbulent diffusivity profile
K_c	turbulent diffusivity for liquid water drops
K_H	turbulent diffusivity for sensible heat
K_M	turbulent diffusivity for momentum
K_χ	turbulent diffusivity for moisture vapor
L	Monin-Obukhov scale length
L_v	latent heat of vaporization
P	ambient atmospheric pressure
R_N	net all-wavelength radiation
$\mathrm{RH}_i(1)$	initial relative humidity at the 1 m level
S	spray rate per meter of line
T	ambient temperature
T_A	absolute temperature
$T_i(1)$	initial ambient temperature at the 1 m level
T_0	temperature at the height z_0
T_*	similarity temperature profile coefficient
U	upstream solution node
UU	midpoint between vertically adjacent upstream nodes
$W(z)$	weighting function for initial water droplet distribution
α_H	ratio of turbulent diffusivity of sensible heat to the turbulent diffusivity of momentum
α_0	α_H at the height z_0
ζ	dimensionless height ratio $[=z/L]$
ζ_0	dimensionless height ratio $[=z_0/L]$
$\Delta\zeta$	solution increment in the ζ direction
ρ	ambient air density
ϕ	general diffusing property

Φ contaminant source term
Φ_c liquid water concentration source term
Φ_H sensible heat source term
Φ_χ water vapor concentration source term
χ ambient water vapor concentration
χ_0 water vapor concentration at the height z_0
χ_s saturated water vapor concentration
χ_* similarity water vapor concentration profile coefficient

REFERENCES

Abramowitz, M., and I. A. Stegun, 1965: *Handbook of Mathematical Functions with Formulas, Graphs, and Mathematical Tables.* U. S. Department of Commerce, National Bureau of Standards, 1046 pp.

Bible, B. B., R. L. Cuthbert and R. L. Carolus, 1968: Response of some vegetable crops to atmospheric modifications under field conditions. *Proc. Amer. Soc. Hort. Sci.*, **92**, 590–594.

Brooks, F. A., 1961: Need for measuring horizontal gradients in determining vertical eddy transfer of heat and moisture. *J. Meteor.*, **18**, 589–596.

Calder, K. L., 1939: A note on the constancy of horizontal turbulent shearing stress in the lower layers of the atmosphere. *Quart. J. Roy. Meteor. Soc.*, **65**, 537–541.

Carolus, R. L., 1967: The control of evapotranspiration in the open by spraying with water: Effect on the quality and yield of fruit and market garden crops. Pepinieristes, Horticulteurs, Maraichers, No. 73, 3889–3891. Tital and abstract in English, *Hort. Abstr.*, 1968, **38**, No. 4, 968, No. 7568.

——, 1969: Evaporative cooling techniques for regulating plant water stress. *Proc. Symp. Amer. Soc. Hort. Sci.*, Pullman, Wash. [Published at a later date as part of: Knott, J. E., *et al.*, 1971: Environmental factors in vegetable production. *Hort. Sci.*, **6**, 21–36.]

——, A. E. Erickson, E. H. Kidder and R. F. Wheaton, 1965: Interaction of climate and soil moisture on water use, growth, and development of tomatoes. *Mich. Agric. Expt. Sta. Quart. Bull.*, **47**, No. 4, 542–581, May 1965. [Copy of the reprint available from Mich. Agric. Expt. Sta. Bull. Office, Michigan State University, E. Lansing, 48824. Abstract available in *Hort. Abstr.*, **36**, 143, No. 1219.]

Esmay, M. L., 1969: *Principles of Animal Environment.* AVI Publ. Co., Inc., 325 pp.

Hamming, R. W., 1962: *Numerical Methods for Scientists and Engineers.* McGraw-Hill, 411 pp.

Harrington, J. B., Jr., 1965: Final report atmospheric pollution by aeroallergens: Meteorological phase (1 March 1962 to 28 February 1965). Vol. II. Atmospheric diffusion of ragweek pollen in urban areas: test ORA project 06342. Ph.D. dissertation, The University of Michigan.

Himmelblau, D. M., 1970: *Process Analysis by Statistical Methods.* Wiley, 463 pp.

Inoue, E., *et al.*, 1958: The aerodynamic measurement of photosynthesis over a nursery of rice plants. *J. Agric. Meteor. Japan*, **14**, 45–53. [English Translation Amer. Meteor. Soc., T-J-14, AF 9(604)-6113.]

Korn, G. A., and T. M. Korn, 1968: *Mathematical Handbook for Scientists and Engineers.* McGraw-Hill, 1130 pp.

Leichtmann, D. L., and S. M. Ponomareva, 1969: On the ratio of the turbulent transfer coefficients for heat and momentum in the surface layer of the atmosphere. *Izv. Atmos. Oceanic Phys.*, **5**, 1245–1250.

Lumley, J. L., and H. A. Panofsky, 1964: *The Structure of Atmospheric Turbulence.* Interscience, 239 pp.

Milburn, R. H., 1957: Theory of evaporating water clouds. *J. Colloid Sci.*, **12**, 378–388.

——, 1958: Theory of turbulent evaporating clouds. *J. Colloid Sci.*, **13**, 114–124.

Monin, A. S., and A. M. Obukhov, 1954: Basic laws of turbulent mixing in the ground layer of the atmosphere. *Izv. Akad. Nauk SSSR, Ser. Geofiz.*, **24**, No. 151, 163–187.

——, and A. M. Yaglom, 1971: *Statistical Fluid Mechanics: Mechanics of Turbulence*, Vol. 1. The MIT Press, 769 pp.

Nurnberger, F. V., 1972: Microenvironmental modification by small water droplet evaporation. Ph.D. dissertation, Michigan State University.

Okuyama, M., and J. T. Zung, 1967: Evaporation-condensation coefficient for small droplets. *J. Chem. Phys.*, **46**, 1580–1585.

Patankar, S. V., and D. B. Spalding, 1968: *Heat and Mass Transfer in Boundary Layers.* C.R.C. Press, 138 pp.

——, and ——, 1970: *Heat and Mass Transfer in Boundary Layers*, 2nd ed. Intertext Books, 230 pp.

Priestley, C. H. B., 1955: Free and forced convection in the atmosphere near the ground. *Quart. J. Roy. Meteor. Soc.*, **81**, 139–143.

Richtmyer, R. D., and K. W. Morton, 1967: *Difference Methods for Initial-Value Problems.* Interscience, 405 pp.

Shaw, R. H., 1967: *Ground Level Climatology.* A symposium presented at the Berkeley meeting of the American Association for the Advancement of Science, December 1965, Publ. No. 86, AAAS, Washington, D.C., 395 pp.

Smith, G. D., 1965: *Numerical Solution of Partial Differential Equations.* Oxford University Press, 179 pp.

Sutton, O. G., 1953: *Micrometeorology.* McGraw-Hill, 333 pp.

Swinbank, W. C., 1964: The exponential wind profile. *Quart. J. Roy. Meteor. Soc.*, **90**, 119–135; discussion (1966) **92**, 416–426.

Tennekes, H., and J. L. Lumley, 1972: *First Course in Turbulence.* The MIT Press, 300 pp.

Van Den Brink, C., and R. L. Carolus, 1965: Removal of atmospheric stresses from plants by overhead sprinkler irrigation. *Mich. Agric. Expt. Sta. Quart. Bull.*, **47**, No. 3, 358–363. [Reprints available from Mich. Agric. Expt. Sta. Bull. Office, Michigan State University].

Waggoner, P. E. *et al.*, 1965: *Agricultural Meteorology. Meteor. Monogr.*, No. 28, Amer. Meteor. Soc., 188 pp.

Wang, J. Y., 1972: *Agricultural Meteorology*, 3rd ed., revised. Milieu Info. Serv., 537 pp.

Yordanov, D. L., 1966: On diffusion from a point source in the atmospheric surface layer. *Izv. Atmos. Oceanic Phys.*, **2**, 348–352.

Zung, J. T., 1967a: Evaporation rate and lifetimes of clouds and sprays in air: The cellular model. *J. Chem. Phys.*, **46**, 2064–2070.

——, 1967b: Evaporation rates and lifetimes of clouds and sprays in air: II. The continuum model. *J. Chem. Phys.*, **47**, 3578–3581.

——, 1968: Evaporation rates and lifetimes of clouds and sprays in air: III. The effects of cloud expansion. *J. Chem. Phys.*, **48**, 5181–5186.